



IMPROVING SEISMIC RESPONSE OF A LOW-RISE REINFORCED CONCRETE BUILDING USING ENERGY DISSIPATING METALLIC DEVICE

J. C. Segovia ⁽¹⁾ and V. I. Fernandez-Davila ⁽²⁾

⁽¹⁾ Research Assistant, Civil Engineering Section, Pontificia Universidad Católica del Perú, jcsegovia@pucp.pe

⁽²⁾ Associate Professor, Civil Engineering Section, Pontificia Universidad Católica del Perú, vfernandezdavila@pucp.edu.pe

Abstract

The results of nonlinear seismic analysis of a five-story building composed of reinforced concrete walls are shown. PERFORM 3D [1] computational program was used for the purpose of carry out the nonlinear seismic analysis of reinforced structure with metallic dissipating device (ADAS) and compare their results with those of non-reinforced structure. To represent the nonlinear behavior of structural elements, the following models has been used: fibers for the walls, and concentrated plasticity bending for beams and columns. The floor slabs behavior were considered as rigid diaphragm elastically in its plane, and that the vertical elements are perfectly embedded in the base of the first floor. For Seismic action, three pairs were used records accelerations. the recommendations of FEMA 356 [2] and the ASCE 41-06 [3] has been taken in account, both for generating the structural model, as well as control the stresses and allowed maximum deformations in the structural elements. The results showed that the lateral displacements at the center of mass (CM) of each floor were reduced by up to 53% (top floor); on the walls of reinforced concrete inelastic deformation of the reinforcing steel it was reduced up to 70% maximum and getting an elastic behavior by shear force. Finally the maximum rotations in beams and columns did not exceed the limit specified by the ASCE 41-06 [3], and verified that the original building will not suffer structural collapse against a rare earthquake.

Keywords: device metallic (ADAS), nonlinear dynamic analysis, reduce structural damage.

1. Introduction

Worldwide-accepted seismic-resistant philosophy states that structures must not collapse due to loads applied by severe earthquakes and that they may present repairable damage after the action of moderate earthquakes. However, there is evidence that many buildings suffer irreparable damage even under minor earthquakes loads, and total collapse during severe earthquakes. Seismic protection systems reduce structural damage through different mechanisms, which can be classified in three groups [4]: passive, semi-active, and active. Passive systems can be further classified into three types: seismic isolators, energy dissipaters, and tuned masses.

Metallic dissipaters were developed in New Zealand at the beginning of the 1970s, and the most well-known models are: Added Damping and Stiffness (ADAS), and Triangular Added Damping and Stiffness (TADAS). They have been successfully utilized in the structural reinforcement of reinforced concrete and steel buildings. In Japan, they were implemented in steel buildings of 5, 9, 15, and more than 15 levels, such as the Oujiseishi Headquarters Building located in Tokyo, which features 15 levels and counts with metallic energy dissipation systems. In Mexico City, the Izazaga building, 12 levels of reinforced concrete frames and masonry walls, was built in 1970 and reinforced in 1990 with ADAS systems; this reinforcement achieved up to 40% reduction in lateral displacements according to a non-linear seismic analysis [5]. Also in Mexico City, the Cardiology Hospital formed by 6 levels of reinforced concrete frames was likewise reinforced using ADAS systems; in this case a significant reduction in lateral displacements was equally verified [6]. In the USA, the first reinforced concrete building with ADAS systems was a 2-story Wells Fargo Bank; this building was constructed in 1967 and originally it possessed a non-ductile structural system until it was reinforced in 1992, achieving a 50% reduction in lateral displacements [7]. In Peru, the first metallic dissipaters utilized in structures were Shear Link (SL) type, developed by Bozzo and Barbat [8], and installed in 2004 at the Casino Mubarak, in Lima.

When a building is subjected to the action of severe seismic movements, a significant amount of energy is transmitted to the structure. The energy gets dissipated through the deformations and damage to the structure.

Eq. (1) represents the differential equation of motion corresponding to a dynamic system with a single degree of freedom (SDOF) subjected to the action of a seismic movement at the base (Fig. 1).

$$m \cdot \ddot{u} + c \cdot \dot{u} + f_s = -m \cdot \ddot{u}_g(t) \quad (1)$$

Where m is the total mass of the system, c is the viscous damping, f_s is the restoring force of the system; Eq. (1) can be expressed in terms of energy distribution through Eq. (2) [9]:

$$E_I = E_k + E_s + E_h + E_v \quad (2)$$

Where E_I , E_k , E_s , E_h , E_v , are the total, kinetic, elastic, hysteretic, and damping energies, respectively. Fig. 2 is a schematic representation of Eq. (2): the red color corresponds to E_h , orange to E_v , blue to E_k , and cyan to E_s . Eq. (2) is also valid for systems with multiple degrees of freedom (MDOF).

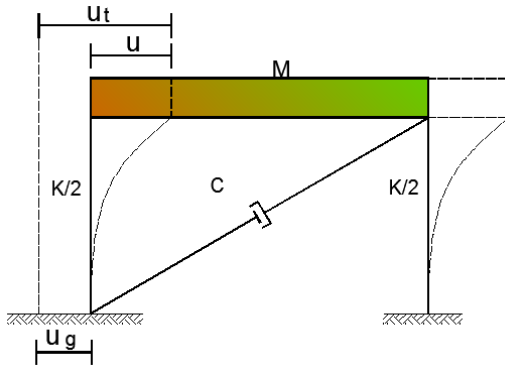


Figure 1 – SDOF Model.

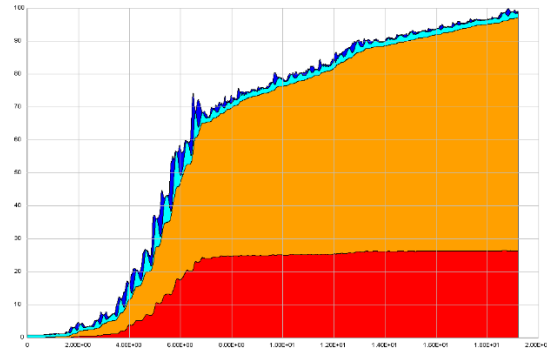
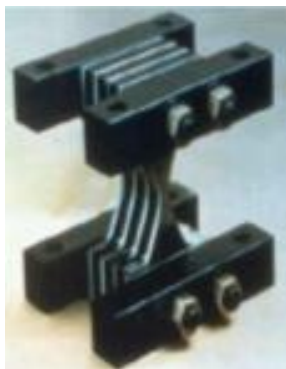


Figure 2 – Energy Input Distribution.

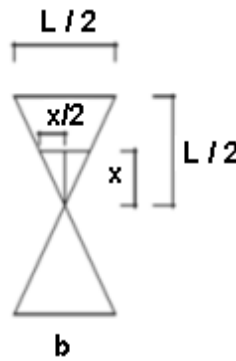
Using energy dissipaters in structures improve their capacity to absorb E_h and E_v energies through supplementary devices, reducing the deformations suffered by beams, columns, and walls, when compared to structures that are not reinforced with this type of system.

2. Properties of ADAS dissipaters

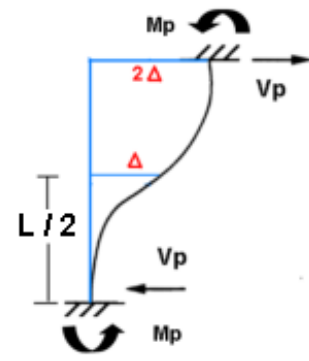
In order to determine the characteristic values of the dissipater's plates geometry, it is feasible to introduce a few idealizations and simplifications [9, 10] (Fig. 3b). The deformation " Δ " can be calculated taking advantage of the sectional symmetry of a plate (Fig. 3c) and using the moment area method, considering a uniform distribution of stresses in all the sections of the dissipater's plates [11] and taking the value of the base as half of its height [9].



a) Real



b) Simplified



c) Lateral deformation

Figure 3 – Characterization of the ADAS dissipater geometry.

$$\Delta = \int_0^{L/2} \frac{M_p \cdot x}{E \cdot I(x)} \cdot dx \quad (3)$$

Where: $M_p = \sigma_y \cdot x \cdot t^2/4$, $I(x) = x^3/12$, and t is the plate's thickness. The lateral displacement Δ is given by:

$$\Delta = \frac{3 \cdot \sigma_y \cdot L^2}{8 \cdot E \cdot t} \quad (4)$$

Finally, the deformation is:

$$\Delta_y^{ADAS} = 2 \cdot \Delta = \frac{3 \cdot \sigma_y \cdot L^2}{4 \cdot E \cdot t} \quad (5)$$

The force V_p on each plate can be calculated from the moment equilibrium at the ends (Fig.3c). For several plates, the value would be equal to V_y or V_p times the number of plates “n” ($V_y = n \cdot V_p$).

$$V_p = V_p^{PI} = \frac{2 \cdot M_p \cdot n}{L} = \frac{\sigma_y \cdot b \cdot t^2 \cdot n}{2 \cdot L} \quad (6)$$

The experimental behavior of ADAS dissipaters subjected to cyclic loads is stable [9]. A bilinear behavior model where the maximum deformation is $\Delta_{Max} = 9 \cdot \Delta_y^{ADAS}$, $K_h = 0.035 \cdot K_d$ (Fig. 4b), $K_d = V_y / \Delta_y^{ADAS}$ yields conservative values lower than the recommended ones [10].

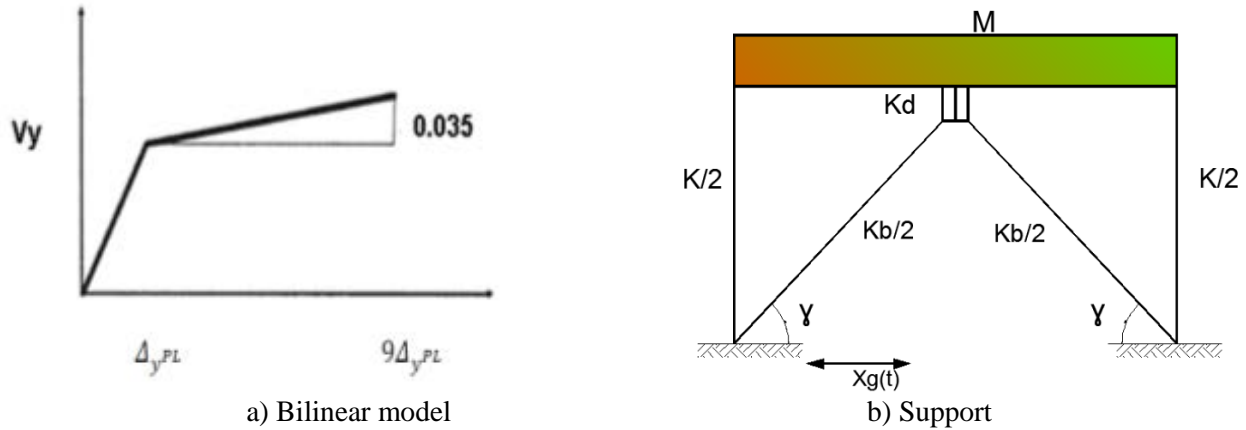


Figure 4 – Properties of the ADAS dissipater.

Support elements are usually Chevron or inverted V braced frames; they should have an adequate resistance [12] recommends that the creep resistance of supports be equal to twice the dissipater force ($F_x = 2V_y$). Considering that the creep stress in the support is σ_y , the horizontal resistance of the supports [12] is:

$$K_{b_{min}} = \frac{2 \cdot V_y \cdot E \cdot \cos \gamma}{\sigma_y \cdot L} \quad (7)$$

3. Modeling of structural elements

3.1 Beams, columns, and dissipater

The non-linear modeling was done through specialized software [1] for tridimensional non-linear structural analysis. The non-linear properties of beams and columns are based on the moment-rotation diagram (Fig. 5a). In Fig. 5b the values of M_y , M_u represent points Y, U, respectively. ASCE-41 [2] Table 2 shows the values of θ at point X for beams and columns, which are similar to those given by FEMA 356 [3].

The analysis did not consider the resistance loss on beams and columns (point R on Fig. 5b) since by then the permissible deformations have been exceeded. The modeling of non-linear behavior in these elements was performed using the concentrated plasticity concept (plastic hinges). The tool [1] defines plastic hinges as “Chord rotation” elements, based on recommendations by FEMA 356 [3].

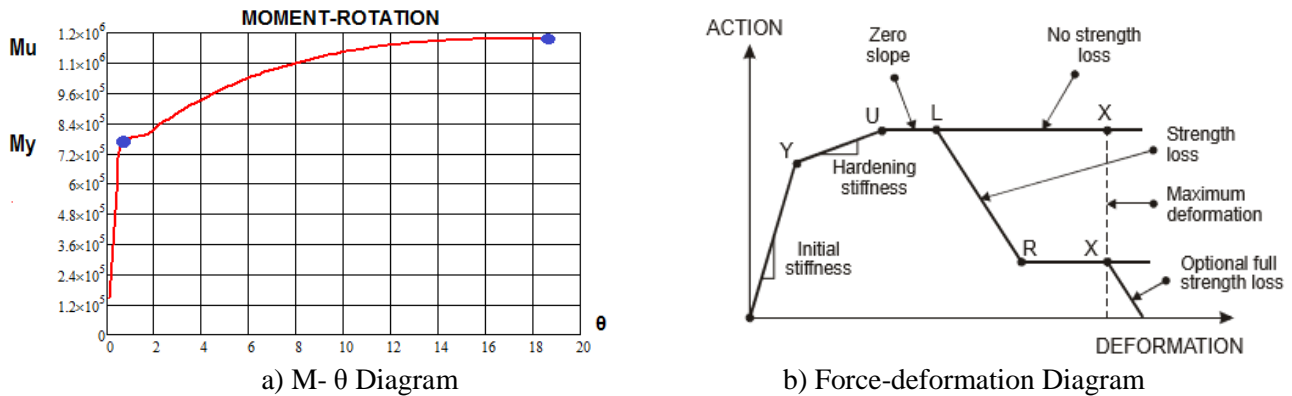


Figure 5 – Moment – Rotation Curve (tri-linear) [1].

Fig. 6 shows the location of plastic hinges in beams and columns. The main points from the $P-M_x-M_y$ interaction diagram [1] are defined for the columns.

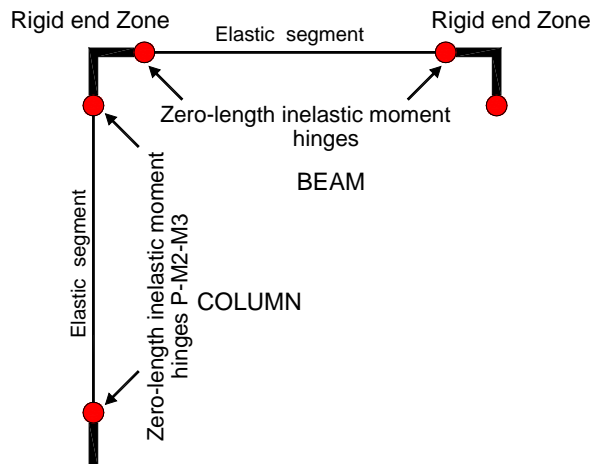


Figure 6 – Location of hinges.

To represent the cyclic degradation on beams, the software [1] uses coefficients [13] and a stiffness degradation factor equal to 0.2 to simulate the behavioral model of Takeda's material [14]. No cyclic degradation was taken into account on the columns since the building mostly contains reinforced concrete walls (Fig. 10) (the percentage of wall area versus total area is 0.8% on H2 and 3% on H1), which mostly work under flexion and shear. Finally, modeling of ADAS dissipaters was done using "Rubber Type" elements [1] calibrated with the bilinear behavior model values shown in Fig. 4a.

3.2 Walls

Fiber elements called "Shear Wall Elements" [15] were used to model walls. The assumptions considered the wall works under flexion loads if $h_w/l_w \geq 1.5$ (Fig. 7), and the behavior under shear loads is linear-elastic. The length of the plastic zone was taken as $l_w/2$ or equal to the height of the first level (whichever is shorter); the effective shear elasticity module (G_e) was considered as equal to $0.25 \cdot G_c$. For modeling purposes, the behavior in the direction perpendicular to the wall's plane was considered to be linear-elastic, with a reduced elasticity module equal to $0.25 \cdot E_c$ due to fissures experienced by the concrete [15].

The software required information on confined concrete, simple concrete, and structural steel for the fiber elements, as well as the stress-deformation relationships of the comprising materials. This was done using a tri-linear model for concrete and steel.

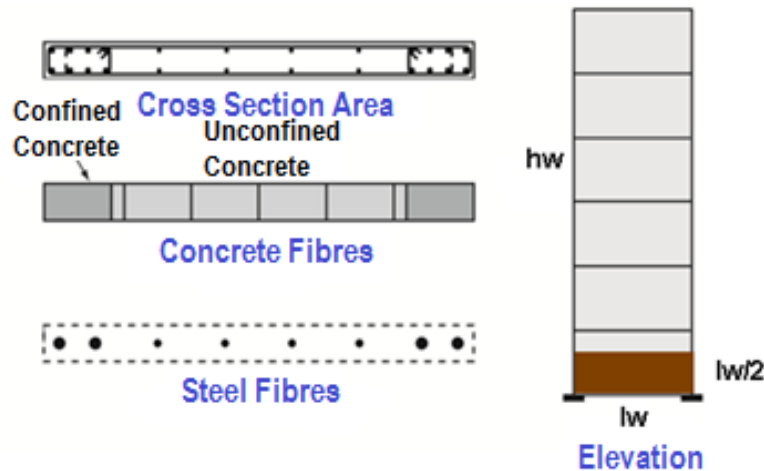


Figure 7 – Fiber-type element used to model the behavior of the walls [16].

Steel values were adjusted to Mander's model [17]; therefore, the ultimate and creep resistances are $f_u = 6300 \text{ kg-f/cm}^2$ and $f_y = 4200 \text{ kg-f/cm}^2$; no cyclic degradation or resistance loss were taken into account. Confined concrete was adjusted to Park's model [18], with a conservative increase of 15% (24.15 MPa) in f'_c (21MPa), and a maximum strain of 0.015. Simple concrete was modeled using 0.019 for strain (maximum resistance) and 0.020 (ultimate resistance). On both concrete models only the resistance loss was taken into account.

4. Seismic logs contemplated

Three paired one-directional acceleration logs were used to determine the non-linear seismic responses of the structure; this is the minimum number suggested by reference [19]. The building is located in Lima (Table 1), and its characteristics are described in reference [20].

Table 1 – Characteristics of the seismic logs used in Lima

ID	Date	Description	PGA (cm/s^2)	PGV (cm/s)	PGD (cm)	Magnitude
S1	17/10/1966	Comp. N82W	180.32	13.23	7.35	7.5
S2	17/10/1966	Comp. N08E	269.5	-21.6	-16.6	7.5
S3	31/05/1970	Comp. L	104.9	4.71	1.55	7.7
S4	31/05/1970	Comp. T	98	6.98	2.64	7.7
S5	03/10/1974	1421 GCT Comp. N08E	178.4	10.3	-5.34	7.5
S6	03/10/1974	1421 GCT Comp. N82W	192.1	14.48	6.41	7.5

4.1 Log scaling

The value of the maximum ground acceleration in the event of a severe earthquake (very rare) is needed to evaluate the seismic behavior of the building. Such earthquake would be the equivalent of the Maximum Considered Earthquake (MCE) given by the norms [19]. This acceleration is calculated through a statistical analysis in areas with a good record of significant earthquakes. The acceleration value (PGA) for rare earthquakes in the coast of Peru is on the order of $0.5 \cdot g$ (480 cm/s^2) [21].

There are two widely used methods to scale the seismic logs (Table 1): a) proportional to the maximum value of the ground acceleration (PGA), and b) the one proposed by the ASCE-07 [19]. Since the structure's maximum periods in both directions are short ($T_1 = 0.51 \text{ s}$, $T_2 = 0.17 \text{ s}$), the response spectrum accelerations of seismic logs in Table 1 were compared to the design spectrum in the Peruvian norm E030 [22] scaled to a single acceleration; the results shown that they have a similar demand for T_1 y T_2 (Fig.8). Finally, the logs were scaled by the proportional method, in such way that the PGA in each log equals $0.5 \cdot g$.

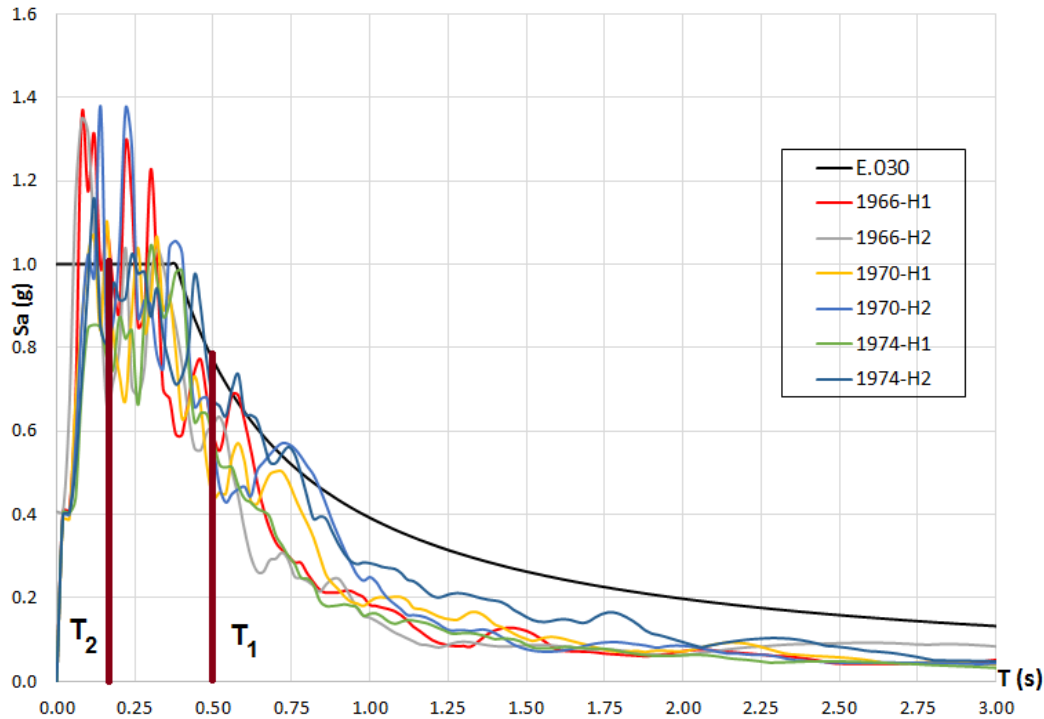


Figure 8 – Response spectra versus E030 design spectra.

5. Evaluation of structural behavior

The evaluation of structural behavior was performed through measurements of rotations, deformations, and shear forces on each structural element, as described below.

5.1 Rotations and deformations.

The rotation and deformation values are summarized in Table 2 given by ASCE 41-06 and values by [16] shown in Fig. 9.

Table 2 – Maximum deformations for structural behavior.

Earthquake load applied	Moderate	Major	Severe
Performance level (damage)	No damage (IO)	Repairable (LS)	No Collapse (CP)
Deformation on Columns (rad.)	$\theta < 0.005$	$\theta < 0.01$	$\theta < 0.02$
Deformation on Beams (rad.)	$\theta < 0.005$	$\theta < 0.01$	$\theta < 0.025$
Drift	0.05	0.01	0.02
Concrete wall (rotations in rad.)	0.03	0.06	0.09

5.1 Shear force.

The walls must present a linear-elastic behavior under shear loads. This is controlled by limiting the shear stress ($V_n/t_w l_w$). Several studies and codes recommend a maximum value, and the most widely used one is $\frac{5}{6}\sqrt{f_c}$ (Mpa) = $10\sqrt{f_c}$ (psi) ACI 318 [23]. V_n can be calculated using the following equation:

$$V_n = A_{cv}(\alpha_c \sqrt{f_c} + \rho_t \cdot f_y) = V_c + V_s \quad (8)$$

Where A_{cv} = cross section area ($t_w l_w$), α_c = coefficient ranging from: 0.17 ($h_w/l_w \geq 2$) $\leq \alpha_c \leq 0.25$ ($h_w/l_w \leq 1.5$) and ρ_t = shear reinforcement value. Shear stress ($V_n/t_w l_w$) was used to verify the shear resistance of the walls (V_n) [1].

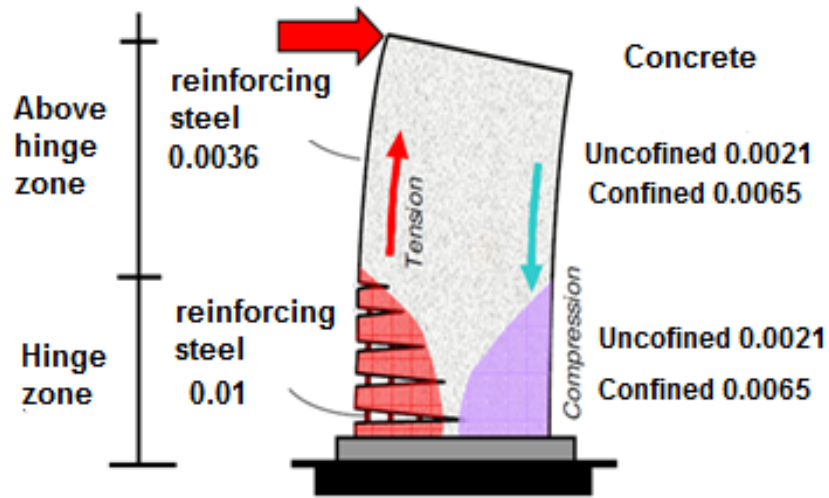


Figure 9 – Controlling wall deformations.
Adapted from [24].

6. Case Study

The building contemplated in this study features five levels and is made of reinforced concrete walls. It was designed for a PGA of 0.4-g, with a reduction factor $R = 4.5$ in both directions by the current norm [22], and a live load equal to 200 kg-f/m^2 . Fig. 10 shows the distribution of structural elements in plan and elevation views; wall thicknesses vary between 0.15 m and 0.20 m.

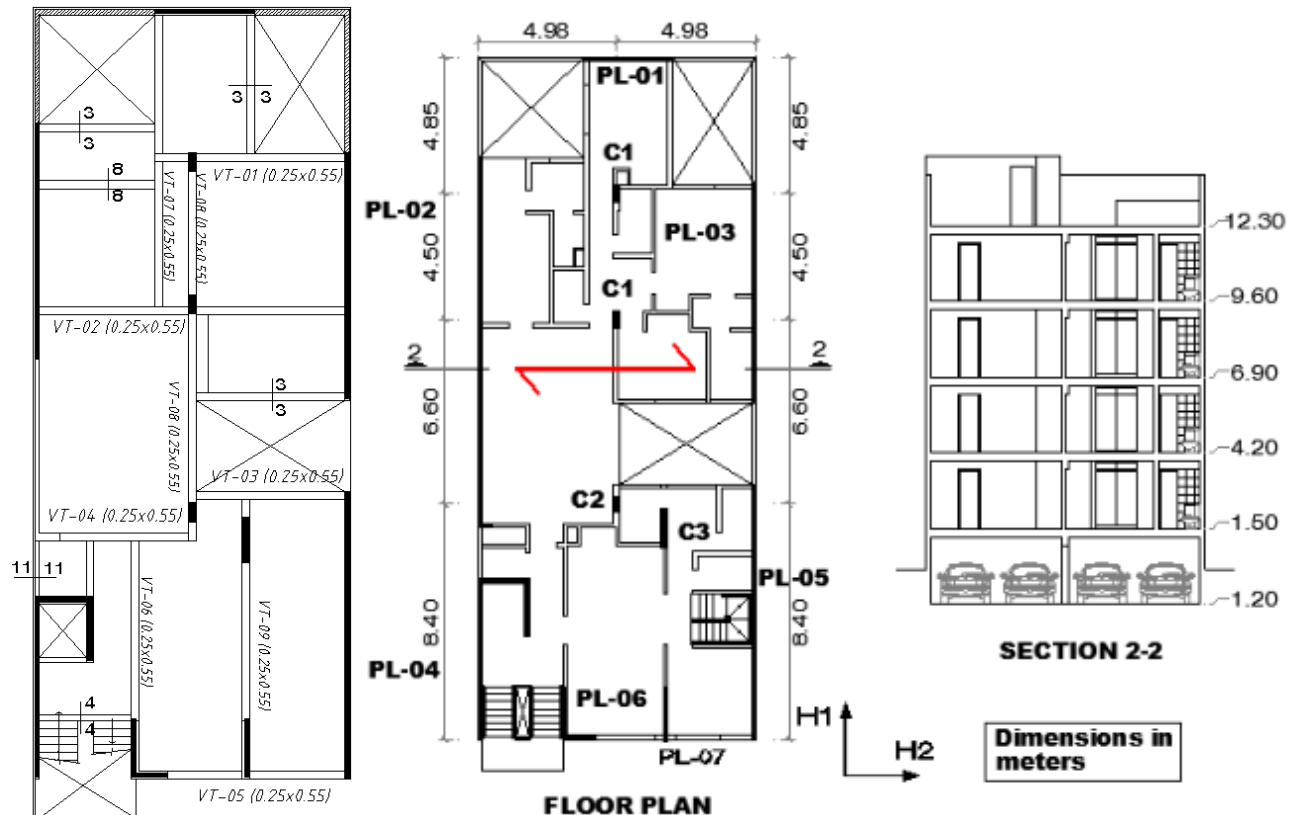


Figure 10 – Characteristics of the low-rise building.

The cylindrical strength of concrete is $f_c' = 21$ MPa (210 kg-f/cm²), and Young's elasticity modulus is $E_c = 217,370.65$ kg-f/cm²; the creep resistance of steel is $f_y = 420$ MPa (4200 kg-f/cm²), and Poisson's coefficient is $\nu = 0.15$. The specific weight of concrete is 2400 kg-f/m³, and the weight per surface unit of partitioning is 1800 kg-f/m². The inertial properties were concentrated in the center of mass (CM) of each level (Table 3), considering a rigid diaphragm with a uniform mass distribution and 5% eccentricity. The structure was modeled using a software [1] to obtain the fundamental vibration periods $T_1 = 0.51$ s (direction H2) and $T_2 = 0.17$ s (direction H1). The viscous damping was taken as the combination of modal damping with $\xi = 5\%$ (low-rise building) and a percentage of Rayleigh's damping (0.2%). The following assumptions were made:

- The time interval for numerical integration was $\Delta t = 0.005$ s.
- Concrete walls behave non-linearly under flexion and elastically under shear loads.
- The torsional stiffnesses of beams, columns, and walls were not taken into account.
- The non-linear behavior of beams and columns under shear loads was not taken into account since it is not critical.
- Axial deformations on beams and columns were not taken into account.

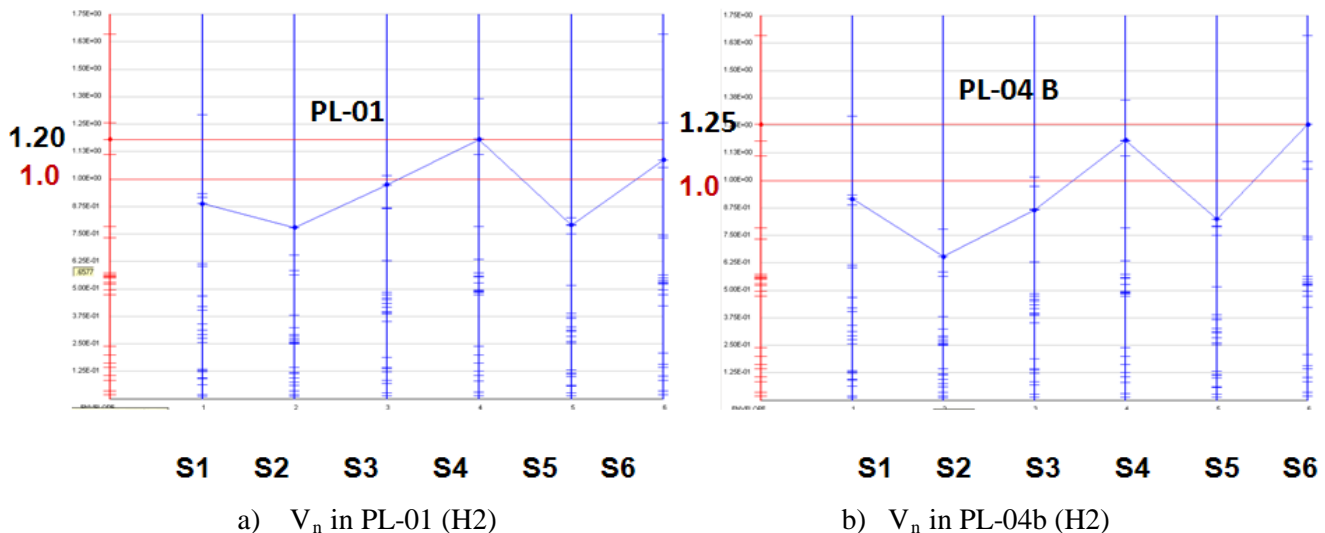
Table 3: Masses used in modeling.

Mass	Levels 1, 2, 3, and 4	Level 5
M_{H1} (kg-f·s ² /m)	21775.8	13167.7
M_{H2} (kg-f·s ² /m)	21775.8	13167.7
MI (kg-f·s ² ·m)	1131094.2	683962.7

6.1 Discussion of the results

The structural behavior was evaluated through the observation of limit deformations (last column in Table 2 and values in Fig. 9) on each structural element. PERFORM 3D greatly simplifies this process and summarizes the results in graphs such as those shown in Fig. 11. This plot illustrates the values of deformations and rotations on a vertical line for different accelerations, scaled to the limit deformations; in other words, a value of 1.0 represents the limit deformation and/or rotation.

Fig.11d shows that not a single element has exceeded the limit deformations on the H1 direction; the largest deformation is V_n in the PL-04 wall. In contrast, in the H2 direction several elements have exceeded the limit deformations, for example: V_n has been exceeded 1.25 times in PL-04B (Fig.11b), 1.20 times in PL-01 (Fig. 11a), and the reinforcement steel deformation has exceeded 1.6 times the permissible value ($0.0058 = 1.6 \cdot 0.0036$) in PL-01 on the zones outside the plastic hinges (Fig. 11c).



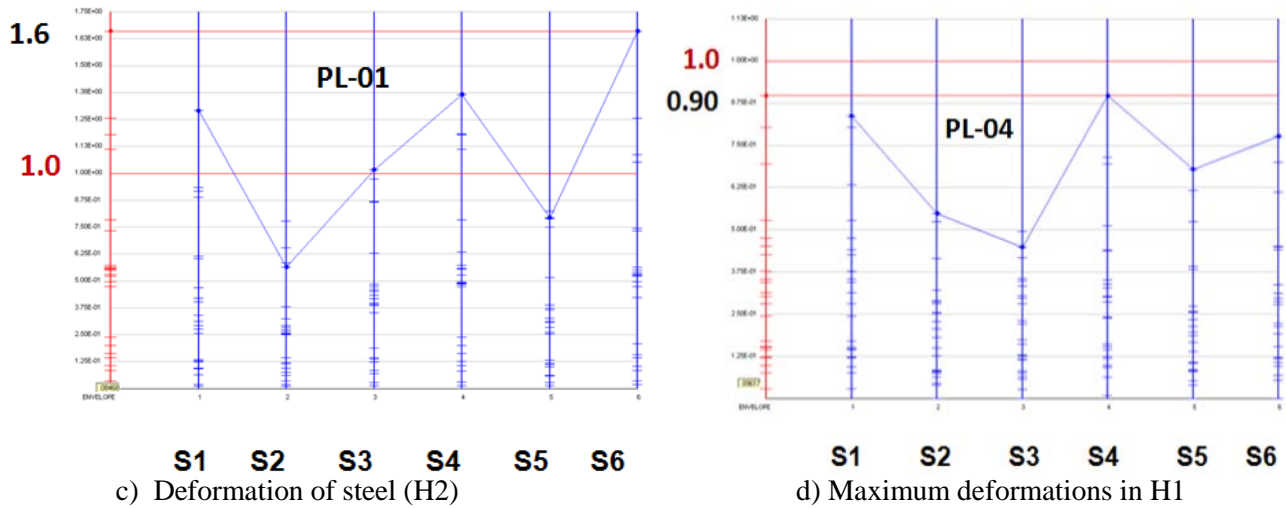


Figure 11 – Maximum deformations.

Deformations and rotations exceeding the limit deformation (1.0 in Fig. 11) are an indication of the presence of difficult or impossible to repair structural damage. To prevent this, the building will be reinforced with ADAS dissipaters in order to keep the deformations and rotations below 1.0.

6.2 Reinforcement using ADAS dissipaters

The dissipaters were designed using an iterative method; successive analyses were performed until the deformations in the elements that showed exceeding values went below the threshold. Fig. 12 shows the location and final dimensions of the dissipaters in axes C and D; these dissipaters have a Chevron layout using W 12x30 profiles verified using Eq. (7). The introduction of the dissipaters reduced the shear force V_n (except in S6 where it exceeds by 14% in PL-04b, which is an acceptable margin), and lowered the deformation in steel and maximum deformations to values below 1.0, as shown in Fig. 13.

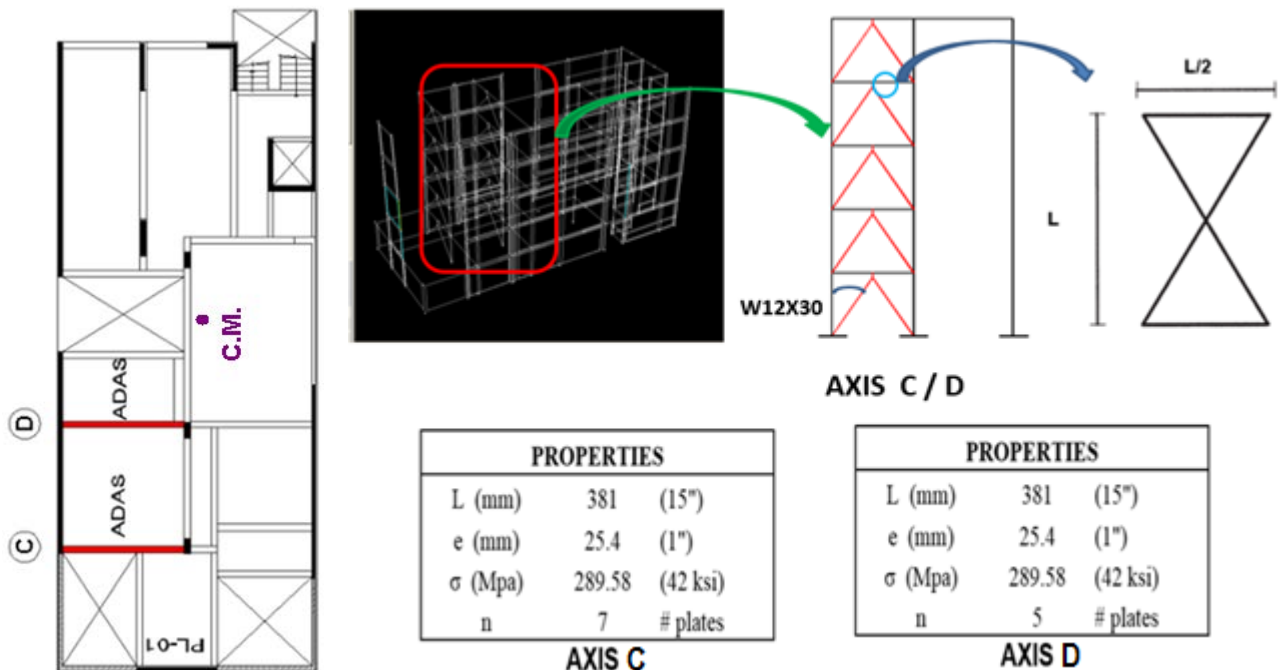


Figure 12 –Reinforcement and final dimensions of ADAS dissipaters in axes C and D.

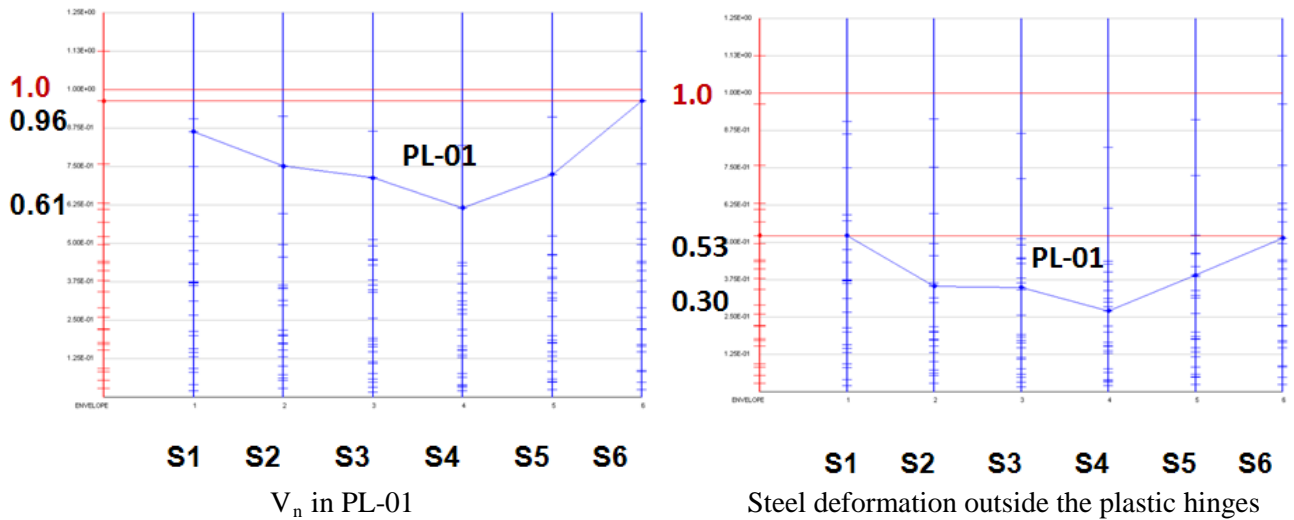


Figure 13 –Final maximum deformations.

The incorporation of ADAS dissipaters reduces the lateral displacements, but they vary according to each earthquake and are smaller at the CM (Figs. 14 and 15).

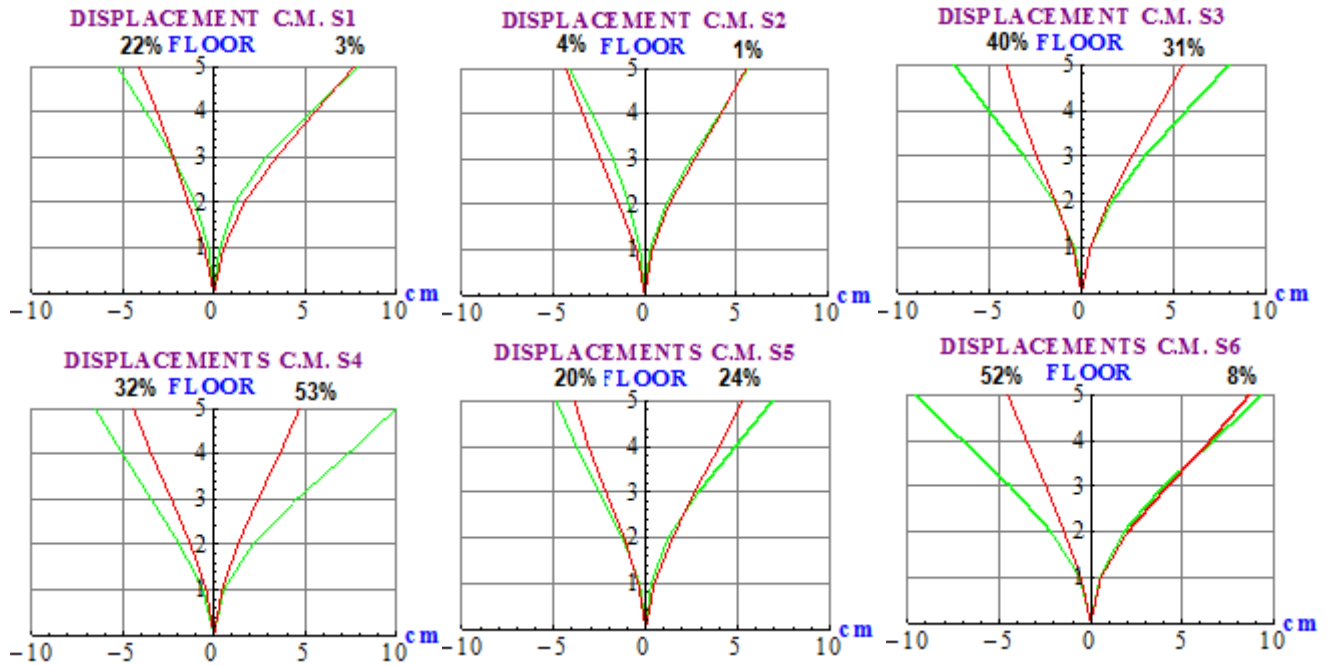
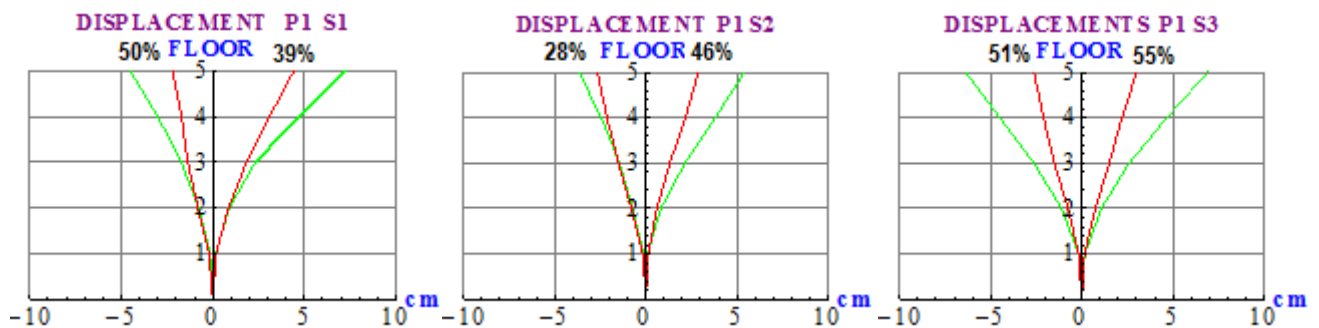


Figure 14 – Comparison of lateral displacements at C.M. (—Original — ADAS)



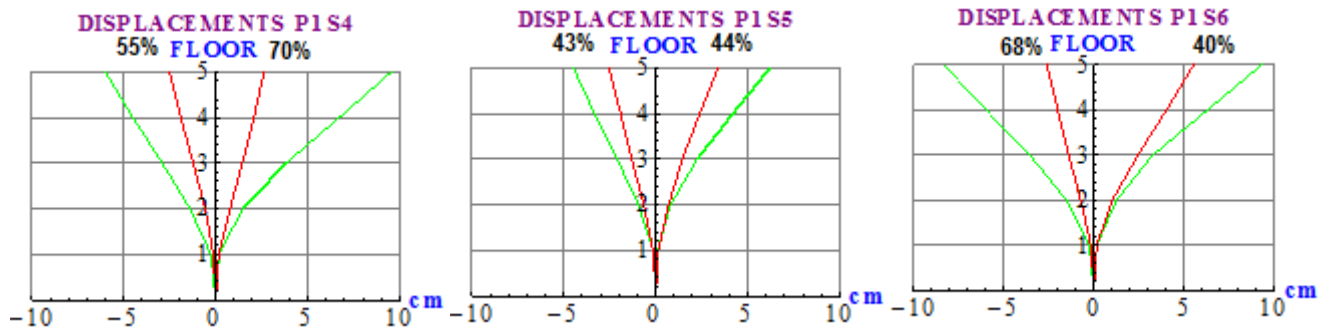


Figure 15 – Comparison of lateral displacements in PL-01(—Original — ADAS).

7. Conclusions

The main conclusions of this study are:

1. The incorporation of ADAS dissipaters in structures subjected to severe earthquakes improves their structural response:
 - Reduction in lateral displacements of up to 53% in the CM at the top level, and up to 70% in PL-01.
 - Reduction in steel deformation of up to 70% in wall PL-01 at the top level, preventing a bending failure.
 - Linear behavior under shear loads on all walls, except for S6 in PL-04b, where it exceeds the allowed value by 14%, which is considered an acceptable margin.
2. The following conclusions can be extracted from the non-linear dynamic analysis performed on the building without dissipaters subjected to a severe earthquake ($PGA = 0.5 \cdot g$):
 - Walls PL-01 and PL-04B behave non-elastically under shear loads; the maximum shear force exceeds by 20% and 25% the maximum allowed, respectively.
 - The deformation of the reinforcement steel in wall PL-01 exceeded by 60% the maximum allowed in zones outside the plastic hinges (second floor).
3. Beams and columns in this building showed maximum rotations of 0.01 radians, below the maximum allowed values (0.02 and 0.025 radians, respectively). This suggests that the structural walls control the seismic response of this building.

8. Acknowledgements

The authors wish to express their gratitude to the Civil Engineering Section of the Postgraduate School at the Pontificia Universidad Católica del Perú.

9. References

- [1] CSI (2011). "PERFORM 3D: Nonlinear Analysis and Performance Assessment for 3D Structures", Version 5, Computers and Structures, Inc., Berkeley, California (Licensee Conceded to PUCP).
- [2] FEMA356 (2000). Washington DC: Federal Emergency Management Agency.
- [3] ASCE 41-06 (2006) Supplement No. 1, American Society of Civil Engineers. ASCE 41-06 Seismic Rehabilitation of Buildings Supplement No. 1.
- [4] Soong T.T., Dargush G.F., (1997). Passive Energy Dissipation Systems in Structural Engineering, Wiley, Chichester, England.
- [5] Sadek, F. Mohraz, B. Taylor, A. W. Chung, R. M. (1996). Passive Energy Dissipation Devices for Seismic Applications NISTIR 5923; 59 p.

- [6] Craig JI, Goodno BJ, Towashiraporn P, Park J., (2002). Response modification applications for essential facilities, Mid-America Earthquake Center Project ST-4 Final Report.
- [7] Perry CL, Fierro EA, Sedarat H, Scholl RE. (1993). Seismic upgrade in San Francisco using energy dissipation devices. *Earthquake Spectra*; 9(3):559–79.
- [8] Bozzo, L. M., Barbat, A.H., (1999). *Diseño Sismorresistente de Edificios*, Editorial Reverte S.A., Barcelona.
- [9] Alonso, L. J. (1989). “Mechanical Characteristics of X-Plate Energy Dissipators.” CE 299 Report, University of California, Berkeley, CA.
- [10] Whittaker, A. S., Bertero, V. V., Alonso L. J. and Thompson, C. L. (1989) " Earthquake simulator testing of steel plate added damping and stiffness elements", Report UCB/EERC-89/02, Earthquake Engineering Research Center, University of California at Berkeley.
- [11] Scholl, R. (1988) *Added Damping and Stiffness Elements for Earthquake Damage and Loss Control*. Proceedings of Conference XLI: A Review of Earthquake Research.
- [12] Su, Y.F. and Hanson, R.D. (1990), "Seismic response of building structures with mechanical damping device", Report No. UMCE 90-2, Department of Civil Engineering, University of Michigan, Ann Arbor, Michigan.
- [13] Naish, D. B. (2010).” Testing and Modeling of Reinforced Concrete Coupling Beams”, Thesis for the degree Doctor of Philosophy in Civil Engineering, University of California Los Angeles.
- [14] Hooper, M. W. (2009)” Analytical Models for the Nonlinear Seismic Response of Reinforced Concrete Frames”, Thesis Master of Science, The Pennsylvania State University The Graduate School College of Engineering.
- [15] Powell, G. (2007). Detailed example of a tall shear wall building using CSI’s Perform 3D nonlinear dynamic analysis. Berkeley, CA: Computers and Structures Inc.
- [16] PEER/ATC (2010). Modeling acceptance criteria for seismic design and analysis of tall buildings (PEER/ATC Report 72-1). Berkeley, CA: Pacific Earthquake Engineering.
- [17] Mander, J.B., Priestley, M.J.N. and Park, R. (1984), *Seismic design of bridge piers*, Research Report 84-2, Department of Civil Engineering, University of Canterbury, New Zealand.
- [18] Park Y. J., Ang A. H-S., and Wen Y. K. (1987). *Damage-Limiting Aseismic Design of Buildings*. *Earthquake Spectra*: February 1987, Vol. 3, No. 1, pp. 1-26.
- [19] ASCE 7-05 (2006). American Society of Civil Engineers. *ASCE 7-05 Minimum Design Loads for Buildings and Other Structures*. Reston, VA.
- [20] Segovia J. C. (2016). *Diseño de disipadores metálicos para una edificación de baja altura de concreto armado*, Tesis de Maestría (en proceso), Pontificia Universidad Católica del Perú, Perú.
- [21] Muñoz P.A., Tinman B. M., Quiun W. D., (2000). “Riesgo Sísmico de Edificios Peruanos”, II Congreso Nacional de Estructuras y Construcción, Lima.
- [22] Reglamento Nacional de Edificaciones. (2007). “Norma Técnica de Edificación E.060 - Concreto Armado”.
- [23] ACI 318-08. (2009). American Concrete Institute. *ACI 318-08 Building Code Requirements for Structural Concrete and Commentary*. Farmington Hills, Mississippi.
- [24] http://www.iitgn.ac.in/seismic-Design/files/ShearWall_IS13920_1993-DCR